PHYSICS LETTERS B

CrossMark

Measurement of the $D \to K^-\pi^+$ strong phase difference in $\psi(3770) \to D^0\overline{D}^0$

BESIII Collaboration

M. Ablikim [a], M.N. Achasov [h,1], X.C. Ai [a], O. Albayrak [d], M. Albrecht [c], D.J. Ambrose [ar], F.F. An [a], Q. An [as], J.Z. Bai [a], R. Baldini Ferroli [s], Y. Ban [ac], D.W. Bennett [r], J.V. Bennett [r], M. Bertani [s], J.M. Bian [aq], E. Boger [v,5], O. Bondarenko [w], I. Boyko [v], S. Braun [an], R.A. Briere [d], H. Cai [az], X. Cai [a], O. Cakir [ak], A. Calcaterra [s], G.F. Cao [a], S.A. Cetin [al], J.F. Chang [a], G. Chelkov [v,2], G. Chen [a], H.S. Chen [a], J.C. Chen [a], M.L. Chen [a], S.J. Chen [aa], X. Chen [a], X.R. Chen [x], Y.B. Chen [a], H.P. Cheng [p], X.K. Chu [ac], Y.P. Chu [a], D. Cronin-Hennessy [aq], H.L. Dai [a], J.P. Dai [a], D. Dedovich [v], Z.Y. Deng [a], A. Denig [u], I. Denysenko [v], M. Destefanis [av,ax], W.M. Ding [ae], Y. Ding [y], C. Dong [ab], J. Dong [a], L.Y. Dong [a], M.Y. Dong [a], S.X. Du [bb], J.Z. Fan [aj], J. Fang [a], S.S. Fang [a], Y. Fang [a], L. Fava [aw,ax], C.Q. Feng [as], C.D. Fu [a], O. Fuks [v,5], Q. Gao [a], Y. Gao [aj], C. Geng [as], K. Goetzen [i], W.X. Gong [a], W. Gradl [u], M. Greco [av,ax], M.H. Gu [a], Y.T. Gu [k], Y.H. Guan [a], L.B. Guo [z], T. Guo [z], Y.P. Guo [u], Z. Haddadi [w], Y.L. Han [a], F.A. Harris [ap], K.L. He [a], M. He [a], Z.Y. He [ab], T. Held [c], Y.K. Heng [a], Z.L. Hou [a], C. Hu [z], H.M. Hu [a], J.F. Hu [an], T. Hu [a], G.M. Huang [e], G.S. Huang [as], H.P. Huang [az], J.S. Huang [n], L. Huang [a], X.T. Huang [ae], Y. Huang [aa], T. Hussain [au], C.S. Ji [as], Q. Ji [a], Q.P. Ji [ab], X.B. Ji [a], X.L. Ji [a], L.L. Jiang [a], L.W. Jiang [az], X.S. Jiang [a], J.B. Jiao [ae], Z. Jiao [p], D.P. Jin [a], S. Jin [a], T. Johansson [ay], A. Julin [aq], N. Kalantar-Nayestanaki [w], X.L. Kang [a], X.S. Kang [ab], M. Kavatsyuk [w], B. Kloss [u], B. Kopf [c], M. Kornicer [ap], W. Kuehn [an], A. Kupsc [ay], W. Lai [a], J.S. Lange [an], M. Lara [r], P. Larin [m], M. Leyhe [c], C.H. Li [a], Cheng Li [as], Cui Li [as], D. Li [q], D.M. Li [bb], F. Li [a], G. Li [a], H.B. Li [a], J.C. Li [a], Jin Li [ad], K. Li [ae], K. Li [l], Lei Li [a], P.R. Li [ao], Q.J. Li [a], T. Li [ae], W.D. Li [a], W.G. Li [a], X.L. Li [ae], X.N. Li [a], X.Q. Li [ab], Z.B. Li [ai], H. Liang [as], Y.F. Liang [ag], Y.T. Liang [an], D.X. Lin [m], B.J. Liu [a], C.L. Liu [d], C.X. Liu [a], F.H. Liu [af], Fang Liu [a], Feng Liu [e], H.B. Liu [k], H.H. Liu [o], H.M. Liu [a], J. Liu [a], J.P. Liu [az], K. Liu [aj], K.Y. Liu [y], P.L. Liu [ae], Q. Liu [ao], S.B. Liu [as], X. Liu [x], Y.B. Liu [ab], Z.A. Liu [a], Zhiqiang Liu [a], Zhiqing Liu [u], H. Loehner [w], X.C. Lou [a,3], G.R. Lu [n], H.J. Lu [p], H.L. Lu [a], J.G. Lu [a], Y. Lu [a], Y.P. Lu [a], C.L. Luo [z], M.X. Luo [ba], T. Luo [ap], X.L. Luo [a], M. Lv [a], X.R. Lyu [ao,*], F.C. Ma [y], H.L. Ma [a], Q.M. Ma [a], S. Ma [a], T. Ma [a], X.Y. Ma [a], F.E. Maas [m], M. Maggiora [av,ax], Q.A. Malik [au], Y.J. Mao [ac], Z.P. Mao [a], J.G. Messchendorp [w], J. Min [a], T.J. Min [a], R.E. Mitchell [r], X.H. Mo [a], Y.J. Mo [e], H. Moeini [w], C. Morales Morales [m], K. Moriya [r], N.Yu. Muchnoi [h,1], H. Muramatsu [aq], Y. Nefedov [v], F. Nerling [m], I.B. Nikolaev [h,1], Z. Ning [a], S. Nisar [g], X.Y. Niu [a], S.L. Olsen [ad], Q. Ouyang [a], S. Pacetti [t], M. Pelizaeus [c], H.P. Peng [as], K. Peters [i], J.L. Ping [z], R.G. Ping [a], R. Poling [aq], M. Qi [aa], S. Qian [a], C.F. Qiao [ao], L.Q. Qin [ae], N. Qin [az], X.S. Qin [a], Y. Qin [ac], Z.H. Qin [a], J.F. Qiu [a], K.H. Rashid [au], C.F. Redmer [u], M. Ripka [u], G. Rong [a], X.D. Ruan [k], A. Sarantsev [v,4], K. Schoenning [ay], S. Schumann [u], W. Shan [ac], M. Shao [as], C.P. Shen [b], X.Y. Shen [a], H.Y. Sheng [a], M.R. Shepherd [r], W.M. Song [a], X.Y. Song [a], S. Spataro [av,ax], B. Spruck [an], G.X. Sun [a], J.F. Sun [n], S.S. Sun [a], Y.J. Sun [as], Y.Z. Sun [a], Z.J. Sun [a], Z.T. Sun [as], C.J. Tang [ag], X. Tang [a], I. Tapan [am], E.H. Thorndike [ar], M. Tiemens [w], D. Toth [aq], M. Ullrich [an], I. Uman [al],

G.S. Varner [ap], B. Wang [ab], D. Wang [ac], D.Y. Wang [ac], K. Wang [a], L.L. Wang [a], L.S. Wang [a],
M. Wang [ae], P. Wang [a], P.L. Wang [a], Q.J. Wang [a], S.G. Wang [ac], W. Wang [a], X.F. Wang [aj],
Y.D. Wang [s], Y.F. Wang [a], Y.Q. Wang [u], Z. Wang [a], Z.G. Wang [a], Z.H. Wang [as], Z.Y. Wang [a],
D.H. Wei [j], J.B. Wei [ac], P. Weidenkaff [u], S.P. Wen [a], M. Werner [an], U. Wiedner [c], M. Wolke [ay],
L.H. Wu [a], N. Wu [a], Z. Wu [a], L.G. Xia [aj], Y. Xia [q], D. Xiao [a], Z.J. Xiao [z], Y.G. Xie [a], Q.L. Xiu [a],
G.F. Xu [a], L. Xu [a], Q.J. Xu [l], Q.N. Xu [ao], X.P. Xu [ah], Z. Xue [a], L. Yan [as], W.B. Yan [as], W.C. Yan [as],
Y.H. Yan [q], H.X. Yang [a], L. Yang [az], Y. Yang [e], Y.X. Yang [j], H. Ye [a], M. Ye [a], M.H. Ye [f], B.X. Yu [a],
C.X. Yu [ab], H.W. Yu [ac], J.S. Yu [x], S.P. Yu [ae], C.Z. Yuan [a], W.L. Yuan [aa], Y. Yuan [a], A. Yuncu [al],
A.A. Zafar [au], A. Zallo [s], S.L. Zang [aa], Y. Zeng [q], B.X. Zhang [a], B.Y. Zhang [a], C. Zhang [aa],
C.B. Zhang [q], C.C. Zhang [a], D.H. Zhang [a], H.H. Zhang [ai], H.Y. Zhang [a], J.J. Zhang [a], J.Q. Zhang [a],
J.W. Zhang [a], J.Y. Zhang [a], J.Z. Zhang [a], S.H. Zhang [a], X.J. Zhang [a], X.Y. Zhang [ae], Y. Zhang [a],
Y.H. Zhang [a], Z.H. Zhang [e], Z.P. Zhang [as], Z.Y. Zhang [az], G. Zhao [a], J.W. Zhao [a], Lei Zhao [as],
Ling Zhao [a], M.G. Zhao [ab], Q. Zhao [a], Q.W. Zhao [a], S.J. Zhao [bb], T.C. Zhao [a], X.H. Zhao [aa],
Y.B. Zhao [a], Z.G. Zhao [as], A. Zhemchugov [v,5], B. Zheng [at], J.P. Zheng [a], Y.H. Zheng [ao],
B. Zhong [z], L. Zhou [a], Li Zhou [ab], X. Zhou [az], X.K. Zhou [ao], X.R. Zhou [as], X.Y. Zhou [a], K. Zhu [a],
K.J. Zhu [a], X.L. Zhu [aj], Y.C. Zhu [as], Y.S. Zhu [a], Z.A. Zhu [a], J. Zhuang [a], B.S. Zou [a], J.H. Zou [a]

a *Institute of High Energy Physics, Beijing 100049, People's Republic of China*
b *Beihang University, Beijing 100191, People's Republic of China*
c *Bochum Ruhr-University, D-44780 Bochum, Germany*
d *Carnegie Mellon University, Pittsburgh, PA 15213, USA*
e *Central China Normal University, Wuhan 430079, People's Republic of China*
f *China Center of Advanced Science and Technology, Beijing 100190, People's Republic of China*
g *COMSATS Institute of Information Technology, Defence Road, Off Raiwind Road, 54000 Lahore, Pakistan*
h *G.I. Budker Institute of Nuclear Physics SB RAS (BINP), Novosibirsk 630090, Russia*
i *GSI Helmholtzcentre for Heavy Ion Research GmbH, D-64291 Darmstadt, Germany*
j *Guangxi Normal University, Guilin 541004, People's Republic of China*
k *GuangXi University, Nanning 530004, People's Republic of China*
l *Hangzhou Normal University, Hangzhou 310036, People's Republic of China*
m *Helmholtz Institute Mainz, Johann-Joachim-Becher-Weg 45, D-55099 Mainz, Germany*
n *Henan Normal University, Xinxiang 453007, People's Republic of China*
o *Henan University of Science and Technology, Luoyang 471003, People's Republic of China*
p *Huangshan College, Huangshan 245000, People's Republic of China*
q *Hunan University, Changsha 410082, People's Republic of China*
r *Indiana University, Bloomington, IN 47405, USA*
s *INFN Laboratori Nazionali di Frascati, I-00044, Frascati, Italy*
t *INFN and University of Perugia, I-06100, Perugia, Italy*
u *Johannes Gutenberg University of Mainz, Johann-Joachim-Becher-Weg 45, D-55099 Mainz, Germany*
v *Joint Institute for Nuclear Research, 141980 Dubna, Moscow region, Russia*
w *KVI, University of Groningen, NL-9747 AA Groningen, The Netherlands*
x *Lanzhou University, Lanzhou 730000, People's Republic of China*
y *Liaoning University, Shenyang 110036, People's Republic of China*
z *Nanjing Normal University, Nanjing 210023, People's Republic of China*
aa *Nanjing University, Nanjing 210093, People's Republic of China*
ab *Nankai university, Tianjin 300071, People's Republic of China*
ac *Peking University, Beijing 100871, People's Republic of China*
ad *Seoul National University, Seoul, 151-747 Korea*
ae *Shandong University, Jinan 250100, People's Republic of China*
af *Shanxi University, Taiyuan 030006, People's Republic of China*
ag *Sichuan University, Chengdu 610064, People's Republic of China*
ah *Soochow University, Suzhou 215006, People's Republic of China*
ai *Sun Yat-Sen University, Guangzhou 510275, People's Republic of China*
aj *Tsinghua University, Beijing 100084, People's Republic of China*
ak *Ankara University, Dogol Caddesi, 06100 Tandogan, Ankara, Turkey*
al *Dogus University, 34722 Istanbul, Turkey*
am *Uludag University, 16059 Bursa, Turkey*
an *Universitaet Giessen, D-35392 Giessen, Germany*
ao *University of Chinese Academy of Sciences, Beijing 100049, People's Republic of China*
ap *University of Hawaii, Honolulu, HI 96822, USA*
aq *University of Minnesota, Minneapolis, MN 55455, USA*
ar *University of Rochester, Rochester, NY 14627, USA*
as *University of Science and Technology of China, Hefei 230026, People's Republic of China*
at *University of South China, Hengyang 421001, People's Republic of China*
au *University of the Punjab, Lahore-54590, Pakistan*
av *University of Turin, I-10125, Turin, Italy*
aw *University of Eastern Piedmont, I-15121, Alessandria, Italy*
ax *INFN, I-10125, Turin, Italy*
ay *Uppsala University, Box 516, SE-75120 Uppsala, Sweden*
az *Wuhan University, Wuhan 430072, People's Republic of China*
ba *Zhejiang University, Hangzhou 310027, People's Republic of China*
bb *Zhengzhou University, Zhengzhou 450001, People's Republic of China*

A B S T R A C T

We study $D^0\overline{D}^0$ pairs produced in e^+e^- collisions at $\sqrt{s} = 3.773$ GeV using a data sample of 2.92 fb^{-1} collected with the BESIII detector. We measured the asymmetry $\mathcal{A}_{K\pi}^{CP}$ of the branching fractions of $D \to K^-\pi^+$ in CP-odd and CP-even eigenstates to be $(12.7 \pm 1.3 \pm 0.7) \times 10^{-2}$. $\mathcal{A}_{K\pi}^{CP}$ can be used to extract the strong phase difference $\delta_{K\pi}$ between the doubly Cabibbo-suppressed process $\overline{D}^0 \to K^-\pi^+$ and the Cabibbo-favored process $D^0 \to K^-\pi^+$. Using world-average values of external parameters, we obtain $\cos\delta_{K\pi} = 1.02 \pm 0.11 \pm 0.06 \pm 0.01$. Here, the first and second uncertainties are statistical and systematic, respectively, while the third uncertainty arises from the external parameters. This is the most precise measurement of $\delta_{K\pi}$ to date.

1. Introduction

Within the Standard Model, the short-distance contribution to D^0–$\overline{D}^0$ oscillations is highly suppressed by the GIM mechanism [1] and by the magnitude of the CKM matrix elements [2] involved. However, long distance effects, which cannot be reliably calculated, will also affect the size of mixing. Studies of D^0–$\overline{D}^0$ oscillation provide knowledge of the size of these long-distance effects and, given improved calculations, can contribute to searches for new physics [3]. In addition, improved constraints on charm mixing are important for studies of CP violation (CPV) in charm physics.

Charm mixing is described by two dimensionless parameters

$$x = 2\frac{M_1 - M_2}{\Gamma_1 + \Gamma_2} \qquad y = \frac{\Gamma_1 - \Gamma_2}{\Gamma_1 + \Gamma_2},$$

where $M_{1,2}$ and $\Gamma_{1,2}$ are the masses and widths of the two mass eigenstates in the D^0-$\overline{D}^0$ system. The most precise determination of the mixing parameters comes from the measurement of the time-dependent decay rate of the wrong-sign process $D^0 \to K^+\pi^-$. These analyses are sensitive to $y' \equiv y\cos\delta_{K\pi} - x\sin\delta_{K\pi}$ and $x' \equiv x\cos\delta_{K\pi} + y\sin\delta_{K\pi}$ [4], where $\delta_{K\pi}$ is the strong phase difference between the doubly Cabibbo-suppressed (DCS) amplitude for $\overline{D}^0 \to K^-\pi^+$ and the corresponding Cabibbo-favored (CF) amplitude for $D^0 \to K^-\pi^+$. In particular,

$$\frac{\langle K^-\pi^+|\overline{D}^0\rangle}{\langle K^-\pi^+|D^0\rangle} = -re^{-i\delta_{K\pi}}, \tag{1}$$

where

$$r = \left| \frac{\langle K^-\pi^+|\overline{D}^0\rangle}{\langle K^-\pi^+|D^0\rangle} \right|.$$

Knowledge of $\delta_{K\pi}$ is important for extracting x and y from x' and y'. In addition, a more accurate $\delta_{K\pi}$ contributes to precision determinations of the CKM unitarity angle ϕ_3[6] via the ADS method [5].

Using quantum-correlated techniques, $\delta_{K\pi}$ can be accessed in the mass-threshold production process $e^+e^- \to D^0\overline{D}^0$ [6]. In this process, D^0 and $\overline{D}^0$ are in a C-odd quantum-coherent state where the two mesons necessarily have opposite CP eigenvalues [3]. Thus,

threshold production provides a unique way to identify the CP of one neutral D by probing the decay of the partner D. Because CPV in D decays is very small compared with the mixing parameters, we will assume no CPV in our analysis. In this paper, we often refer to $K^-\pi^+$ only for simplicity, but charge-conjugate modes are always implied when appropriate.

We denote the asymmetry of CP-tagged D decay rates to $K^-\pi^+$ as

$$\mathcal{A}_{K\pi}^{CP} \equiv \frac{\mathcal{B}_{D^{S-} \to K^-\pi^+} - \mathcal{B}_{D^{S+} \to K^-\pi^+}}{\mathcal{B}_{D^{S-} \to K^-\pi^+} + \mathcal{B}_{D^{S+} \to K^-\pi^+}}, \tag{2}$$

where $S+$ ($S-$) denotes the CP-even (CP-odd) eigenstate. To lowest order in the mixing parameters, we have the relation [7,8]

$$2r\cos\delta_{K\pi} + y = (1 + R_{WS}) \cdot \mathcal{A}_{K\pi}^{CP}, \tag{3}$$

where R_{WS} is the decay rate ratio of the wrong sign process $\overline{D}^0 \to K^-\pi^+$ (including the DCS decay and D mixing followed by the CF decay) and the right sign process $D^0 \to K^-\pi^+$ (i.e., the CF decay). Here, D^0 or $\overline{D}^0$ refers to the state at production. Using external values for the parameters r, y, and R_{WS}, we can extract $\delta_{K\pi}$ from $\mathcal{A}_{CP \to K\pi}$.

We use the D-tagging method [9] to obtain the branching fractions $\mathcal{B}_{D^{S\pm} \to K^-\pi^+}$ as

$$\mathcal{B}_{D^{S\pm} \to K^-\pi^+} = \frac{n_{K^-\pi^+,S\pm}}{n_{S\pm}} \cdot \frac{\varepsilon_{S\pm}}{\varepsilon_{K^-\pi^+,S\pm}}. \tag{4}$$

Here, $n_{S\pm}$ and $\varepsilon_{S\pm}$ are yields and detection efficiencies of single tags (ST) of $S\pm$ final states, while $n_{K^-\pi^+,S\pm}$ and $\varepsilon_{K^-\pi^+,S\pm}$ are yields and efficiencies of double tags (DT) of ($S\pm$, $K^-\pi^+$) final states, respectively. Based on an 818 pb^{-1} data sample collected with the CLEO-c detector at $\sqrt{s} = 3.77$ GeV and a more complex analysis technique, the CLEO Collaboration obtained $\cos\delta_{K\pi} = 0.81^{+0.22+0.07}_{-0.18-0.05}$ [8]. Using a global fit method including external inputs for mixing parameters, CLEO obtained $\cos\delta_{K\pi} = 1.15^{+0.19+0.00}_{-0.17-0.08}$ [8].

In this paper, we present a measurement of $\delta_{K\pi}$, using the quantum correlated productions of D^0–$\overline{D}^0$ mesons at $\sqrt{s} = 3.773$ GeV in e^+e^- collisions with an integrated luminosity of 2.92 fb^{-1} [10] collected with the BESIII detector [11].

2. The BESIII detector

The Beijing Spectrometer (BESIII) views e^+e^- collisions in the double-ring collider BEPCII. BESIII is a general-purpose detector [11] with 93% coverage of the full solid angle. From the interaction point (IP) to the outside, BESIII is equipped with a main drift chamber (MDC) consisting of 43 layers of drift cells, a time-of-flight (TOF) counter with double-layer scintillator in the barrel part and single-layer scintillator in the end-cap part, an electromagnetic

---

Table 1
D decay modes used in this analysis.

Type	Mode
Flavored	$K^-\pi^+, K^+\pi^-$
$S+$	$K^+K^-, \pi^+\pi^-, K_S^0\pi^0\pi^0, \pi^0\pi^0, \rho^0\pi^0$
$S-$	$K_S^0\pi^0, K_S^0\eta, K_S^0\omega$

calorimeter (EMC) composed of 6240 CsI(Tl) crystals, a superconducting solenoid magnet providing a magnetic field of 1.0 T along the beam direction, and a muon counter containing multi-layer resistive plate chambers installed in the steel flux-return yoke of the magnet. The MDC spatial resolution is about 135 μm and the momentum resolution is about 0.5% for a charged track with transverse momentum of 1 GeV/c. The energy resolution for showers in the EMC is 2.5% at 1 GeV. More details of the spectrometer can be found in Ref. [11].

3. MC simulation

Monte Carlo (MC) simulation serves to estimate the detection efficiency and to understand background components. MC samples corresponding to about 10 times the luminosity of data are generated with a GEANT4-based [12] software package [13], which includes simulations of the geometry of the spectrometer and interactions of particles with the detector materials. KKMC is used to model the beam energy spread and the initial-state radiation (ISR) in the e^+e^- annihilations [14]. The inclusive MC samples consist of the production of $D\overline{D}$ pairs with consideration of quantum coherence for all modes relevant to this analysis, the non-$D\overline{D}$ decays of $\psi(3770)$, the ISR production of low mass ψ states, and QED and $q\bar{q}$ continuum processes. Known decays recorded in the Particle Data Group (PDG) [15] are simulated with EVTGEN [16] and the unknown decays with LUNDCHARM [17]. The final-state radiation (FSR) off charged tracks is taken into account with the PHOTOS package [18]. MC samples of $D \to S\pm, \overline{D} \to X$ (X denotes inclusive decay products) processes are used to estimate the ST efficiencies, and MC samples of $D \to S\pm, \overline{D} \to K\pi$ processes are used to estimate the DT efficiencies.

4. Data analysis

The decay modes used for tagging the CP eigenstates are listed in Table 1, where $\pi^0 \to \gamma\gamma$, $\eta \to \gamma\gamma$, $K_S^0 \to \pi^+\pi^-$ and $\omega \to \pi^+\pi^-\pi^0$. For each mode, D candidates are reconstructed from all possible combinations of final-state particles, according to the following selection criteria.

Momenta and impact parameters of charged tracks are measured by the MDC. Charged tracks are required to satisfy $|\cos\theta| < 0.93$, where θ is the polar angle with respect to the beam axis, and have a closest approach to the IP within ± 10 cm along the beam direction and within ± 1 cm in the plane perpendicular to the beam axis. Particle identification is implemented by combining the information of normalized energy deposition (dE/dx) in the MDC and the flight time measurements from the TOF. For a charged $\pi(K)$ candidate, the probability of the $\pi(K)$ hypothesis is required to be larger than that of the $K(\pi)$ hypothesis.

Photons are reconstructed as energy deposition clusters in the EMC. The energies of photon candidates must be larger than 25 MeV for $|\cos\theta| < 0.8$ (barrel) and 50 MeV for $0.84 < |\cos\theta| < 0.92$ (end-cap). To suppress fake photons due to electronic noise or beam backgrounds, the shower time must be less than 700 ns from the event start time [19]. However, in the case that no charged track is detected, the event start time is not reliable, and instead the shower time must be within ± 500 ns from the time of the most energetic shower.

Table 2
Requirements on ΔE for different D reconstruction modes.

Mode	Requirement (GeV)
K^+K^-	$-0.025 < \Delta E < 0.025$
$\pi^+\pi^-$	$-0.030 < \Delta E < 0.030$
$K_S^0\pi^0\pi^0$	$-0.080 < \Delta E < 0.045$
$\pi^0\pi^0$	$-0.080 < \Delta E < 0.040$
$\rho^0\pi^0$	$-0.070 < \Delta E < 0.040$
$K_S^0\pi^0$	$-0.070 < \Delta E < 0.040$
$K_S^0\eta$	$-0.040 < \Delta E < 0.040$
$K_S^0\omega$	$-0.050 < \Delta E < 0.030$
$K^\pm\pi^\mp$	$-0.030 < \Delta E < 0.030$

Our π^0 and η candidates are selected from pairs of photons with the requirement that at least one photon candidate reconstructed in the barrel is used. The mass windows imposed are 0.115 GeV/c^2 < $m_{\gamma\gamma}$ < 0.150 GeV/c^2 for π^0 candidates and 0.505 GeV/c^2 < $m_{\gamma\gamma}$ < 0.570 GeV/c^2 for η candidates. We further constrain the invariant mass of each photon pair to the nominal π^0 or η mass, and update the four momentum of the candidate according to the fit results.

The K_S^0 candidates are reconstructed via $K_S^0 \to \pi^+\pi^-$ using a vertex-constrained fit to all pairs of oppositely charged tracks, with no particle identification requirements. These tracks have a looser IP requirement: their closest approach to the IP is required to be less than 20 cm along the beam direction, with no requirement in the transverse plane. The χ^2 of the vertex fit is required to be less than 100. In addition, a second fit is performed, constraining the K_S^0 momentum to point back to the IP. The flight length, L, obtained from this fit must satisfy $L/\sigma_L > 2$, where σ_L is the estimated error on L. Finally, the invariant mass of the $\pi^+\pi^-$ pair is required to be within $(0.487, 0.511)$ GeV/c^2, which corresponds to three times the experimental mass resolution.

4.1. Single tags using CP modes

For the CP-even and CP-odd modes, the two variables beam-constrained mass M_{BC} and energy difference ΔE are used to identify the signals, defined as follows:

$$M_{BC} \equiv \sqrt{E_{beam}^2/c^4 - |\vec{p}_D|^2/c^2},$$

$$\Delta E \equiv E_D - E_{beam}.$$

Here $\vec{p}_D$ and E_D are the total momentum and energy of the D candidate, and E_{beam} is the beam energy. Signals peak around the nominal D mass in M_{BC} and around zero in ΔE. Boundaries of ΔE requirements are set at approximately $\pm 3\sigma$, except that those of modes containing a π^0 are set as $(-4\sigma, +3.5\sigma)$ due to the asymmetric distributions. In each event, only the combination of D candidates with the least $|\Delta E|$ is kept per mode.

In the K^+K^- and $\pi^+\pi^-$ modes, backgrounds of cosmic rays and Bhabha events are removed with the following requirements. First, the two charged tracks used as the CP tag must have a TOF time difference less than 5 ns and they must not be consistent with being a muon pair or an electron–positron pair. Second, there must be at least one EMC shower (other than those from the CP tag tracks) with an energy larger than 50 MeV or at least one additional charged track detected in the MDC. In the $K_S^0\pi^0$ mode, backgrounds due to $D^0 \to \rho\pi$ are negligible after restricting the decay length of K_S^0 with $L/\sigma_L > 2$. In the $\rho^0\pi^0$ and $K_S^0\omega$ modes, mass ranges of 0.60 GeV/c^2 < $m_{\pi^+\pi^-}$ < 0.95 GeV/c^2 and 0.72 GeV/c^2 < $m_{\pi^+\pi^-\pi^0}$ < 0.84 GeV/c^2 are required for identifying ρ and ω candidates, respectively.
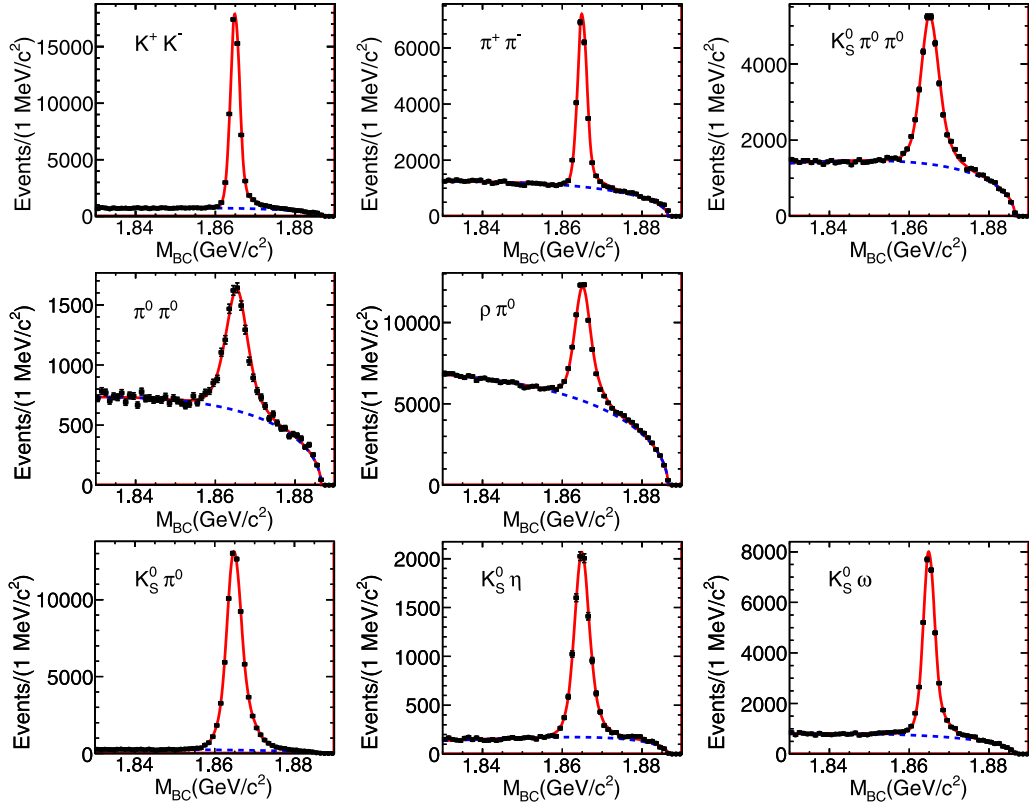
Fig. 1. The M_{BC} distributions of the single-tag (ST) *CP* modes. Data are shown as points with error bars. The solid lines are the total fits and the dashed lines are the background contribution.

Table 3

Yields and efficiencies of all single-tag (ST) and double-tag (DT) modes. First, we list the ST (*CP* mode) yields ($n_{S\pm}$) and corresponding efficiencies ($\varepsilon_{S\pm}$) and then the DT mode yields ($n_{K\pi,S\pm}$) and efficiencies ($\varepsilon_{K\pi,S\pm}$). Uncertainties are statistical only.

ST mode	$n_{S\pm}$	$\varepsilon_{S\pm}(\%)$
K^+K^-	$56\,156\pm261$	62.99 ± 0.26
$\pi^+\pi^-$	$20\,222\pm187$	65.58 ± 0.26
$K_S^0\pi^0\pi^0$	$25\,156\pm235$	16.46 ± 0.07
$\pi^0\pi^0$	7610 ± 156	42.77 ± 0.21
$\rho\pi^0$	$41\,117\pm354$	36.22 ± 0.21
$K_S^0\pi^0$	$72\,710\pm291$	41.95 ± 0.21
$K_S^0\eta$	$10\,046\pm121$	35.12 ± 0.20
$K_S^0\omega$	$31\,422\pm215$	17.88 ± 0.10

DT mode	$n_{K\pi,S\pm}$	$\varepsilon_{K\pi,S\pm}(\%)$
$K\pi,\ K^+K^-$	1671 ± 41	42.33 ± 0.21
$K\pi,\ \pi^+\pi^-$	610 ± 25	44.02 ± 0.21
$K\pi,\ K_S^0\pi^0\pi^0$	806 ± 29	12.86 ± 0.13
$K\pi,\ \pi^0\pi^0$	213 ± 14	30.42 ± 0.18
$K\pi,\ \rho\pi^0$	1240 ± 35	25.48 ± 0.16
$K\pi,\ K_S^0\pi^0$	1689 ± 41	29.06 ± 0.17
$K\pi,\ K_S^0\eta$	230 ± 15	24.84 ± 0.16
$K\pi,\ K_S^0\omega$	747 ± 27	12.60 ± 0.06

After applying the criteria on ΔE in Table 2 in all the *CP* modes, we plot their M_{BC} distributions in Fig. 1, where the peaks at the nominal D^0 mass are evident. Maximum likelihood fits to the events in Fig. 1 are performed, where in each mode the signals are modeled with the reconstructed signal shape in MC simulation convoluted with a smearing Gaussian function, and backgrounds are modeled with the ARGUS function [20]. The Gaussian functions are supposed to compensate for the resolution differences between data and MC simulation. Based on the fit results, the es-timated yields of the *CP* modes are given in Table 3, along with their MC-determined detection efficiencies.

4.2. Double tags of the $K^-\pi^+$ and CP modes

In the surviving ST *CP* modes, we reconstruct $D \to K^-\pi^+$ among the unused charged tracks. The $D \to K^-\pi^+$ candidate must pass the ΔE requirement listed in Table 2; in the case of multiple candidates, the one with the smallest $|\Delta E|$ is chosen. The DT signals peak at the nominal D^0 mass in both $M_{BC}(S\pm)$ and $M_{BC}(K\pi)$. To extract the signal yields, two-dimensional maximum likelihood fits to the distributions of $M_{BC}(S\pm)$ vs. $M_{BC}(K\pi)$ are performed. The signal shapes are derived from MC simulations, and the background shapes contain continuum background and mis-partitioning background where some final-state particles are interchanged between the D^0 and $\overline{D}^0$ candidates in the reconstruction process. Fig. 2 shows an example of the results for one sample DT combination, $(K\pi, K_S^0\pi^0)$. Table 3 lists the yields of the DT modes and their corresponding detection efficiencies as determined with MC simulations.

5. Purities of the *CP* modes

It is necessary to determine the *CP*-purity of our ST modes. For the $K_S^0\pi^0$ ($K_S^0\eta$) mode, the issue is the background under the K_S^0 peak. We use the sideband regions of the K_S^0 mass, $[0.470, 0.477]$ GeV/c^2 and $[0.521, 0.528]$ GeV/c^2, in the $m_{\pi^+\pi^-}$ distributions, to estimate the backgrounds from $\pi^+\pi^-\pi^0$ ($\pi^+\pi^-\eta$). The purity is estimated to be 98.5% (almost 100%) for the $K_S^0\pi^0$ ($K_S^0\eta$) mode. For the $K_S^0\omega$, $K_S^0\pi^0\pi^0$ and $\rho^0\pi^0$ modes, due to the complexity of the involved non-resonant and resonant processes, we evaluate the *CP*-purity directly from our data.

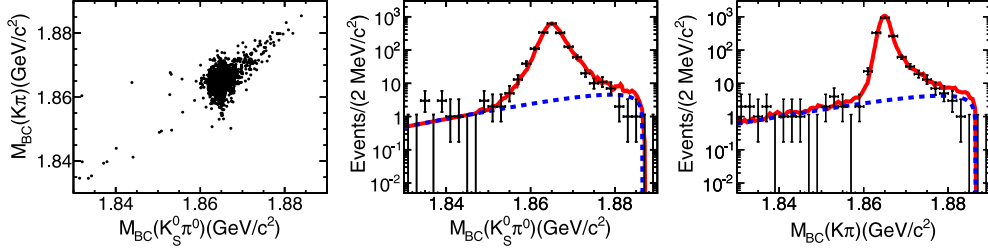*BESIII Collaboration / Physics Letters B 734 (2014) 227–233*

Fig. 2. An illustration of our DT yield analysis, using the $K\pi$, $K_S^0\pi^0$ mode. A scatter plot (left) of the two M_{BC} values is displayed, along with projections of the two-dimensional fit to the same data (middle and right). The solid lines are the total fits and the dashed lines are the background contribution.

Table 4

The same-*CP* yields and the corresponding efficiencies used in our *CP*-purity tests. The uncertainties are statistical only. The last column presents the obtained f_S and numbers in the parentheses are the lower limits of the f_S at 90% confidence level.

Mode (S', S)	$n_{S',S}$	$\varepsilon_{S',S}$ (%)	f_S (%)
K^+K^-, $K_S^0\pi^0\pi^0$	8 ± 3	11.80 ± 0.11	91.6 ± 16.7 (> 86.8)
K^+K^-, $\rho^0\pi^0$	13 ± 8	24.44 ± 0.16	84.0 ± 12.6 (> 70.6)
$K_S^0\pi^0$, $K_S^0\omega$	7 ± 3	6.77 ± 0.08	94.6 ± 8.0 (> 90.6)

We use additional DT combinations, with a clean *CP*-tag in combination with the mode we wish to study. We look for signals where both *D* mesons decay with equal *CP* eigenvalue. If *CP* is conserved, the same-*CP* process is prohibited in the quantum-correlated $D\bar{D}$ production at threshold, unless our studied *CP* modes are not pure. If we take f_S as the fraction of the right *CP* components in the *CP* tag mode, we have the yields of the same-*CP* process written as

$$n_{S',S} = (1 - f_S) \cdot n_S \cdot \mathcal{B}_{D \to S'} \cdot \varepsilon_{S',S}/\varepsilon_S,$$

where mode S' is chosen to be (nearly) pure in its *CP* eigenstate.

We take the modes $K_S^0\pi^0$ ($S'-$) and K^+K^- ($S'+$) as our clean *CP* tags to test the $S-$ and $S+$ purities of our ST modes, respectively. We analyze our data to find (S', S) events using selection criteria similar to those described in Section 4.2. However, a simplified procedure is used to obtain the yields. We implement a one-dimensional fit to the $M_{BC}(S)$ distributions for the signal mode *S* of interest, while restricting the $M_{BC}(S')$ distributions for the tagging modes S' in the signal region 1.860 GeV/$c^2 <$ $M_{BC}(K^+K^-) < 1.875$ GeV/c^2 and 1.855 GeV/$c^2 < M_{BC}(K_S^0\pi^0) <$ 1.880 GeV/c^2. The DT signals are described with the signal MC shape convoluted with a Gaussian function, and backgrounds are modeled with the ARGUS function. Fig. 3 shows the $M_{BC}(S)$ distributions in the DT events and the fits to the distributions. Table 4 lists the DT yields and the corresponding detection efficiencies. In the tested *CP* modes, the observed numbers of the same-*CP* events are quite small and nearly consistent with zero, which indicates that f_S is close to 1. This one-dimensional fit may let certain peaking backgrounds survive; however, an over-estimated $n_{S',S}$ leads to a more conservative evaluation of f_S.

6. Systematic uncertainties

In calculating $\mathcal{A}_{K\pi}^{CP}$, uncertainties of most of efficiencies cancel out, such as those for tracking, particle identification and $\pi^0/\eta/K_S^0$ reconstruction. The efficiency differences $\Delta_{S\pm} = \Delta(\frac{\varepsilon_{S\pm}}{\varepsilon_{K\pi,S\pm}})$ of $K^-\pi^+$ between data and MC simulation are studied for the modes $S\pm$. We use control samples to study $\Delta_{S\pm}$. The $K^-\pi^+$ final state is used for studying $\Delta_{S\pm}$ in the K^+K^- and $\pi^+\pi^-$ modes; $K^-\pi^+\pi^0$ is used for the $\pi^0\pi^0$, $\rho\pi^0$, $K_S^0\pi^0$ and $K_S^0\eta$ modes; $K^-\pi^+\pi^0\pi^0$ is used for the $K_S^0\pi^0\pi^0$ mode; and $K^+\pi^-\pi^-\pi^+$ is used for the $K_S^0\omega$ mode. We determine $\Delta_{S\pm}$ in different *CP*-tag modes by comparing the ratio of the DT yields to the ST yields between data and

MC. We find that $\Delta_{S\pm}$ are at 1% level for different *CP*-tag modes. In the formula of $\mathcal{A}_{K\pi}^{CP}$, the dependence of $\Delta_{S\pm}$ on the *CP* mode is not canceled out. The resulting systematic uncertainty on $\mathcal{A}_{K\pi}^{CP}$ is 0.2×10^{-2}.

Some systematics arise from effects which act among several *CP* modes simultaneously. The efficiency of the cosmic and Bhabha veto (only for the *KK* and $\pi\pi$ modes) is studied based on the inclusive MC sample. We compare the obtained $\mathcal{A}_{K\pi}^{CP}$ with and without this requirement and take the difference of 0.6×10^{-3} as a systematic uncertainty. For the *CP* modes involving K_S^0, *CP*-violating $K_L^0 \to \pi^+\pi^-$ decays are also considered. Using the known branching fraction, we find this causes the change on $\mathcal{A}_{K\pi}^{CP}$ to be 0.8×10^{-3}.

Other systematic uncertainties, relevant to $\mathcal{A}_{K\pi}^{CP}$, are listed in Table 5, which are uncorrelated among different *CP* modes.

The ΔE requirements are mode-dependent. We study possible biases of our requirements by changing their values; we take the maximum variations of the resultant $\mathcal{B}_{D^{S\pm} \to K\pi}$ as systematic uncertainties.

Fitting the M_{BC} distributions involves knowledge of detector smearing and the effects of initial-state and final-state radiation. In the case of ST fits, we scan the smearing parameters within the errors determined in our nominal fits. The maximum changes to $n_{S\pm}$ are taken as a systematic uncertainty. For the DT fits, we obtain checks on $n_{K\pi,S\pm}$ with one-dimensional fits to $M_{BC}(S)$ with inclusion of floating smearing functions. The outcomes of $\mathcal{B}_{D^{S\pm} \to K\pi}$ are consistent with those determined from the two-dimensional fits, and any small differences are treated as systematic uncertainties.

Systematic effects due to the *CP* purities are checked, as stated in Section 5. We introduce the *CP* purities f_S in calculating the $\mathcal{B}_{D^{S\pm} \to K\pi}$ under different *CP* tagging modes and obtain the corrected $\mathcal{B}_{D^{S\pm} \to K\pi}$. We set the lower limits of f_S and take the corresponding maximum changes as part of systematic uncertainties.

7. Results

We combine the branching fractions $\mathcal{B}_{D^{S+} \to K^-\pi^+}$ and $\mathcal{B}_{D^{S-} \to K^-\pi^+}$ in Eq. (4) from two kinds of the *CP* modes based on the standard weighted least-square method [15]. Following Eq. (2), we obtain $\mathcal{A}_{K\pi}^{CP} = (12.7 \pm 1.3 \pm 0.7) \times 10^{-2}$, where the first uncertainty is statistical and the second is systematic. The mode-dependent systematics are propagated to $\mathcal{A}_{K\pi}^{CP}$ and combined with the mode-correlated systematics. The values of $\mathcal{A}_{K\pi}^{CP}$ obtained for the 15 different *CP* mode combinations are also checked as listed in Table 6. Within statistical uncertainties, they are consistent with each other.

With external inputs of $r^2 = (3.50 \pm 0.04) \times 10^{-3}$, $y = (6.7 \pm 0.9) \times 10^{-3}$ from HFAG [21] and $R_{WS} = (3.80 \pm 0.05) \times 10^{-3}$ from PDG [15], $\cos\delta_{K\pi}$ is determined to be $1.02 \pm 0.11 \pm 0.06 \pm 0.01$, where the third uncertainty is due to the errors introduced from the external inputs.
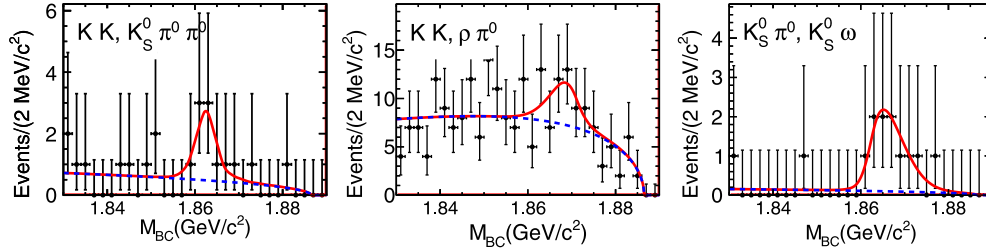
Fig. 3. The M_{BC} distributions from our *CP*-purity tests using same-*CP* processes (S', S), with fits to the total (solid) and background (dashed) contributions. Both S and S' are *CP* eigenstates of D decays.

Table 5
A summary of mode-dependent fractional systematic uncertainties, in percent. A "–" means the systematic uncertainty is negligible.

Source	K^+K^-	$\pi^+\pi^-$	$K_S^0\pi^0\pi^0$	$\pi^0\pi^0$	$\rho^0\pi^0$	$K_S^0\pi^0$	$K_S^0\eta$	$K_S^0\omega$
ΔE requirement	0.6	0.5	0.9	0.7	1.8	0.7	0.5	1.5
Fitting	0.9	1.0	1.5	1.7	0.2	0.1	0.8	2.0
CP purity	–	–	1.8	–	3.5	0.6	–	1.2
Quadratic sum	1.1	1.1	2.5	1.8	3.9	0.9	0.9	2.8

Table 6
Values of $\mathcal{A}_{K\pi}^{CP}$ in units of 10^{-2} extracted from the 15 different combinations of CP decay modes. The errors shown are statistical only.

CP−	*CP*+				
	K^+K^-	$\pi^+\pi^-$	$K_S^0\pi^0\pi^0$	$\pi^0\pi^0$	$\rho\pi^0$
$K_S^0\pi^0$	13.8 ± 1.8	14.5 ± 2.4	10.0 ± 2.3	8.0 ± 3.7	12.2 ± 2.0
$K_S^0\eta$	15.5 ± 3.5	16.3 ± 3.9	11.8 ± 3.8	9.7 ± 4.8	14.0 ± 3.6
$K_S^0\omega$	13.5 ± 2.2	14.2 ± 2.8	9.7 ± 2.7	7.7 ± 3.9	11.9 ± 2.4

8. Summary

We employ a *CP* tagging technique to analyze a sample of 2.92 fb^{-1} quantum-correlated data of $e^+e^- \to D^0\overline{D}^0$ at the $\psi(3770)$ peak. We measure the asymmetry $\mathcal{A}_{K\pi}^{CP} = (12.7 \pm 1.3 \pm 0.7) \times 10^{-2}$. Using the inputs of r^2 and y from HFAG [21] and R_{WS} from PDG [15], we obtain $\cos\delta_{K\pi} = 1.02 \pm 0.11 \pm 0.06 \pm 0.01$. The first uncertainty is statistical, the second is systematic, and the third is due to the external inputs. Our result is consistent with previous results from CLEO [8]. Our result is the most precise to date, and helps to constrain the D^0–$\overline{D}^0$ mixing parameters and the angle ϕ_3 in the unitarity triangle of the CKM matrix.

References

[1] S.L. Glashow, J. Illiopoulos, L. Maiani, Phys. Rev. D 2 (1970) 1285;
R.L. Kingsley, S.B. Treiman, F. Wilczek, A. Zee, Phys. Rev. D 11 (1975) 1919.
[2] N. Cabibbo, Phys. Rev. Lett. 10 (1963) 531;
M. Kobayashi, T. Maskawa, Prog. Theor. Phys. 49 (1973) 652.
[3] S. Bianco, F.L. Fabbri, D. Benson, I. Bigi, Riv. Nuovo Cimento 26 (7) (2003) 1.
[4] L.M. Zhang, et al., Belle Collaboration, Phys. Rev. Lett. 96 (2006), 151801;
B. Aubert, et al., BaBar Collaboration, Phys. Rev. Lett. 98 (2007), 211802;
T. Aaltonen, et al., CDF Collaboration, Phys. Rev. Lett. 100 (2008), 121802.
[5] D. Atwood, I. Dunietz, A. Soni, Phys. Rev. Lett. 78 (1997) 3257;
D. Atwood, I. Dunietz, A. Soni, Phys. Rev. D 63 (2001), 036005.
[6] D. Atwood, A.A. Petrov, Phys. Rev. D 71 (2005), 054032;
D.M. Asner, W.M. Sun, Phys. Rev. D 73 (2006), 034024;
D.M. Asner, W.M. Sun, Phys. Rev. D 77 (2008) 019901 (Erratum);
X.-D. Cheng, K.-L. He, H.-B. Li, Y.-F. Wang, M.-Z. Yang, Phys. Rev. D 75 (2007), 094019.
[7] Z.-Z. Xing, Phys. Rev. D 55 (1997) 196;
H.-B. Li, M.-Z. Yang, Phys. Rev. D 74 (2006), 094016;
M. Gronau, Y. Grossman, J.L. Rosner, Phys. Lett. B 508 (2001) 37.
[8] D.M. Asner, et al., CLEO Collaboration, Phys. Rev. D 86 (2012), 112001.
[9] R.M. Baltrusaitis, et al., MARK-III Collaboration, Phys. Rev. Lett. 56 (1986) 2140;
J. Adler, et al., MARK-III Collaboration, Phys. Rev. Lett. 60 (1988) 89.
[10] M. Ablikim, et al., BESIII Collaboration, Chin. Phys. C 37 (2013), 123001.
[11] M. Ablikim, et al., BESIII Collaboration, Nucl. Instrum. Methods Phys. Res., Sect. A, Accel. Spectrom. Detect. Assoc. Equip. 614 (2010) 345.
[12] S. Agostinelli, et al., GEANT4 Collaboration, Nucl. Instrum. Methods Phys. Res., Sect. A, Accel. Spectrom. Detect. Assoc. Equip. 506 (2003) 250.
[13] Z. Deng, et al., PoS ACAT (2007), 043.
[14] S. Jadach, B.F.L. Ward, Z. Was, Phys. Rev. D 63 (2001), 113009.
[15] J. Beringer, et al., Particle Data Group, Phys. Rev. D 86 (2012), 010001.
[16] D.J. Lange, Nucl. Instrum. Methods Phys. Res., Sect. A, Accel. Spectrom. Detect. Assoc. Equip. 462 (2001) 152;
R.G. Ping, Chin. Phys. C 32 (2008) 599.
[17] J.C. Chen, et al., Phys. Rev. D 62 (2000), 034003.
[18] E. Richter-Was, Phys. Lett. B 303 (1993) 163.
[19] Xiang Ma, et al., Chin. Phys. C 32 (2008) 744;
Y. Guan, X.-R. Lu, Y. Zheng, Y.-F. Wang, Chin. Phys. C 38 (2014) 016201.
[20] H. Albrecht, et al., ARGUS Collaboration, Phys. Lett. B 241 (1990) 278.
[21] Heavy Flavor Averaging Group, http://www.slac.stanford.edu/xorg/hfag/charm/.